Cell

SWI/SNF Complex Prevents Lineage Reversion and Induces Temporal Patterning in Neural Stem Cells

Elif Eroglu,[1] Thomas R. Burkard,[1] Yanrui Jiang,[2] Nidhi Saini,[2] Catarina C.F. Homem,[1] Heinrich Reichert,[2] and Juergen A. Knoblich[1,*]

[1]Institute of Molecular Biotechnology of the Austrian Academy of Sciences, Dr. Bohr-Gasse 3, 1030 Vienna, Austria
[2]Biozentrum, University of Basel, Klingelbergstrasse 50, 4056 Basel, Switzerland
*Correspondence: juergen.knoblich@imba.oeaw.ac.at

http://dx.doi.org/10.1016/j.cell.2014.01.053

SUMMARY

Members of the SWI/SNF chromatin-remodeling complex are among the most frequently mutated genes in human cancer, but how they suppress tumorigenesis is currently unclear. Here, we use *Drosophila* neuroblasts to demonstrate that the SWI/SNF component Osa (ARID1) prevents tumorigenesis by ensuring correct lineage progression in stem cell lineages. We show that Osa induces a transcriptional program in the transit-amplifying population that initiates temporal patterning, limits self-renewal, and prevents dedifferentiation. We identify the Prdm protein Hamlet as a key component of this program. Hamlet is directly induced by Osa and regulates the progression of progenitors through distinct transcriptional states to limit the number of transit-amplifying divisions. Our data provide a mechanistic explanation for the widespread tumor suppressor activity of SWI/SNF. Because the Hamlet homologs Evi1 and Prdm16 are frequently mutated in cancer, this mechanism could well be conserved in human stem cell lineages.

INTRODUCTION

Stem cell lineages often contain a transit-amplifying (TA) progenitor pool that multiplies the number of differentiating progeny (Clarke and Fuller, 2006; Hsu and Fuchs, 2012; Lui et al., 2011). Unlike in stem cells, the ability to self-renew has to be limited in TA progenitors to prevent uncontrolled proliferation (Clarke and Fuller, 2006; Goardon et al., 2011; Krivtsov et al., 2006). Understanding the mechanisms that control the progression from unlimited to limited self-renewal and ultimately to differentiation is therefore important for the treatment of stem cell-originated tumors.

Drosophila larval neuroblasts (NBs) are an attractive model for studying lineage progression in stem cells (Brand and Livesey, 2011; Homem and Knoblich, 2012; Reichert, 2011; Weng and Lee, 2011). Invariantly, they generate progeny that can be uniquely identified based on marker expression and the birth order of cells (Brand and Livesey, 2011; Homem and Knoblich, 2012; Reichert, 2011; Weng and Lee, 2011). NBs express the transcription factors (TFs) Deadpan (Dpn), Helix-loop-helix mγ (HLHmγ), and Klumpfuss (Klu) (Bello et al., 2008; Berger et al., 2012; Boone and Doe, 2008; Bowman et al., 2008; San-Juán and Baonza, 2011; Xiao et al., 2012; Zacharioudaki et al., 2012). The TF Pointed (Pnt), however, is only expressed in so-called type II NBs, where it represses the expression of another TF called Asense (Ase) (Zhu et al., 2011). In contrast to the more abundant type I NB lineages, type II NB lineages contain a TA population and are therefore particularly suitable for the analysis of lineage progression. Asymmetric division of type II NBs generates an immature intermediate neural progenitor (imINP) that initially downregulates Dpn, HLHmγ, and Klu. Subsequently, the imINP goes through several maturation steps, first turning on Ase and then reinitiating the expression of the NB-specific TFs Dpn, HLHmγ, and Klu to become a mature INP (mINP) (Bello et al., 2008; Berger et al., 2012; Boone and Doe, 2008; Bowman et al., 2008; Song and Lu, 2011; Xiao et al., 2012; Zacharioudaki et al., 2012). In addition, INPs but not NBs express the TF Earmuff (Erm) (Weng et al., 2010). Subsequently, the INP divides asymmetrically into another INP and a ganglion mother cell (GMC) that generates two postmitotic neurons (Bello et al., 2008; Boone and Doe, 2008; Bowman et al., 2008). In contrast to NBs that divide many times, INPs differentiate after around five rounds of asymmetric divisions. They consecutively express the TFs Dichaete (D), Grainy head (Grh), and Eyeless (Ey), a phenomenon that is called temporal patterning, which is important for timely cell-cycle exit (Bayraktar and Doe, 2013). How this transcriptional clock is established in INPs and how it progresses through distinct stages are currently unclear.

Asymmetric division of type II NBs is controlled by the proteins Brat and Numb that segregate into imINPs during each division. Numb promotes the INP fate by inhibiting the Notch signaling pathway in imINPs (Bowman et al., 2008; Weng and Lee, 2011). Brat can act as a translational inhibitor in other tissues (Harris et al., 2011; Sonoda and Wharton, 2001). *brat* or *numb* mutant type II NBs generate imINPs that fail to mature and ultimately revert to NBs giving rise to transplantable tumors

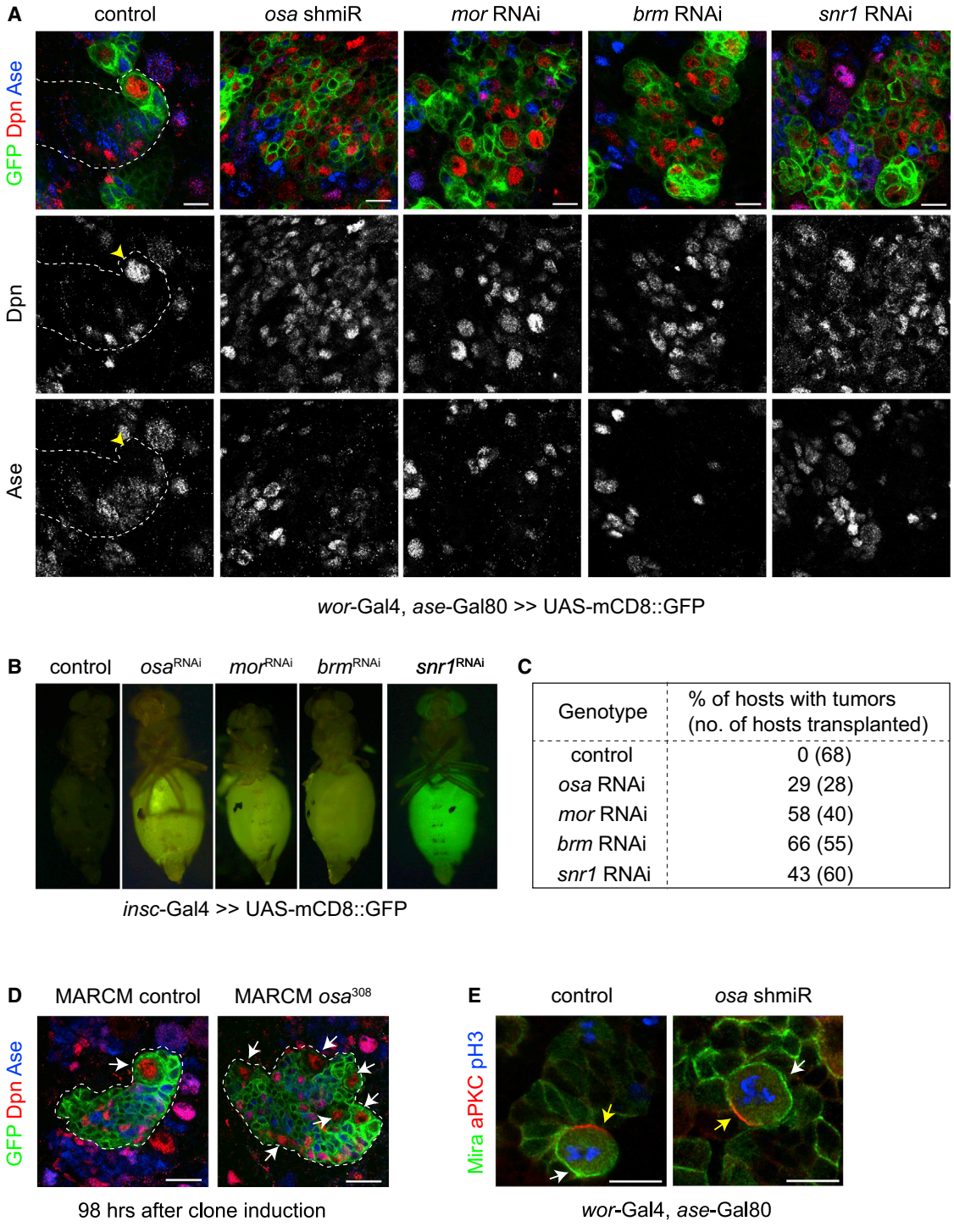

Genotype	% of hosts with tumors (no. of hosts transplanted)
control	0 (68)
osa RNAi	29 (28)
mor RNAi	58 (40)
brm RNAi	66 (55)
snr1 RNAi	43 (60)

Figure 1. Knockdown of SWI/SNF Complex Subunits Causes Transplantable Tumors

(A) Close-up images of larval brains expressing RNAi against *osa*, *mor*, *brm*, or *snr1* in type II lineages, stained for Dpn and Ase. Control type II lineage (outlined) contains a single Dpn$^+$, Ase$^-$ NB (indicated by a yellow arrowhead). RNAi of *osa*, *mor*, *brm*, or *snr1* causes supernumerary Dpn$^+$, Ase$^-$ type II NB-like cells.

(B) GFP$^+$ tissue from larval brains expressing RNAi against *osa*, *mor*, *brm*, or *snr1* transplanted into the abdomens of adult host flies causes tumor formation (green abdomen).

(C) Table showing the frequency of tumor formation 14–28 days after transplantation.

(legend continued on next page)

(Bowman et al., 2008; Caussinus and Gonzalez, 2005). Although the molecular mechanisms that regulate the asymmetric segregation of Brat and Numb are well understood, how their asymmetric distribution is translated into irreversible fate changes in INPs is not clear.

In genome-wide RNAi screens for regulators of NB self-renewal, we identified Osa, Brahma (Brm), Moira (Mor), and Snr1, subunits of the chromatin-remodeling SWI/SNF complex (Neumüller et al., 2011) (unpublished data). Transcriptional changes mediated by the SWI/SNF complex have been implicated in controlling mammalian stem cell self-renewal and differentiation (Ho et al., 2009; Kidder et al., 2009; de la Serna et al., 2006; Lessard and Crabtree, 2010). The complex is also required at different stages of neural development, its functions ranging from the control of neural stem cell self-renewal and proliferation (Lessard et al., 2007; Matsumoto et al., 2006; Seo et al., 2005), to dendritic development and neural circuit formation (Parrish et al., 2006; Tea and Luo, 2011; Wu et al., 2007). Additionally, a recent study shows a critical role for the SWI/SNF complex in modulating direct versus indirect neurogenesis (Tuoc et al., 2013).

Two subtypes of the SWI/SNF complex, BAP and PBAP, have been described in *Drosophila* (Collins et al., 1999; Mohrmann and Verrijzer, 2005). Brm is the core subunit carrying the enzymatic activity; Mor and Snr1 are essential assembly and stability factors (Crosby et al., 1999; Dingwall et al., 1995; Reisman et al., 2009; Tamkun et al., 1992). Osa is a signature subunit, only present in BAP, and is involved in the recruitment of the complex to specific loci (Moshkin et al., 2007; Vázquez et al., 1999). Recently, exome-sequencing studies of primary human tumors identified the mammalian homolog of Osa, ARID1A, as the most frequently mutated SWI/SNF subunit in human cancers (Kadoch et al., 2013; Ronan et al., 2013; Shain and Pollack, 2013), underlining the importance of understanding its role in stem cell lineages.

We identified the protein Hamlet (Ham) as a key target of the SWI/SNF complex in *Drosophila* type II NB lineages. Ham has critical roles in cell fate decisions in external sensory organs (Moore et al., 2002, 2004) and the olfactory system (Endo et al., 2012). Molecularly, Ham is known to induce epigenetic modifications that allow cells to respond to iterative Notch signals (Endo et al., 2012). Ham contains a PR domain that has homology to histone methyltransferases and is the common *Drosophila* homolog of Prdm3/Evi1 and Prdm16, two mammalian Prdm proteins that can act as proto-oncogenes and tumor suppressors in cancer (Fog et al., 2012; Hohenauer and Moore, 2012). A recent report has demonstrated that Evi1 and Prdm16 act redundantly in initiating heterochromatin formation in mammals (Pinheiro et al., 2012).

Here, we use the type II NB lineages to ask how the loss of SWI/SNF activity can lead to tumor formation. We show that loss of Brm, Mor, Snr1, or Osa causes transplantable brain tumors due to dedifferentiation of imINPs to NBs. We identify a transcriptional program activated by Osa in INPs that is required for temporal patterning and self-renewal control. Ham is an integral part of this program. It is required for the progression of temporal patterning in INPs and ensures timely cell-cycle exit. Because Ham is both necessary and sufficient for limiting self-renewal in stem cell lineages, we propose a model where Osa ensures that a self-renewal restriction program is initiated before TA cells resume asymmetric division, and failure to do so leads to the formation of stem cell-derived tumors.

RESULTS

Osa Is a Tumor Suppressor in the *Drosophila* Brain

A genome-wide RNAi screen for defects in NB self-renewal identified the subunits of the SWI/SNF complex: Osa, Mor, and Brm (Neumüller et al., 2011). Another subunit of the complex, Snr1, was identified in an independent screen to cause a similar overproliferation phenotype (Figure S1A available online). Larval brains expressing RNAi against *osa*, *mor*, *brm*, or *snr1* contained additional Dpn$^+$, Ase$^-$ NB-like cells (Figure 1A) and resulted in tumor formation upon transplantation (Figures 1B and 1C), indicating that the tumor suppressor function of SWI/SNF is conserved in *Drosophila*. No tumors were formed upon RNAi of PBAP complex-specific subunits (data not shown), indicating that only the BAP complex controls NB self-renewal. Therefore, we focused on BAP-specific subunit Osa for in-depth analysis.

To confirm the *osa* RNAi phenotype, we used the MARCM system for clonal analysis (Lee and Luo, 1999). Although 98 hr control clones contained only one Dpn$^+$, Ase$^-$ primary NB, *osa* mutant clones contained multiple Dpn$^+$, Ase$^-$ NB-like cells (Figure 1D). This is not due to defects in asymmetric cell division because localization of aPKC, Mira, Numb, and Brat was unaffected (Figures 1E, S1B, and S1C). Similarly, Notch signaling was successfully suppressed in imINPs as revealed by mγ-GFP reporter (Figure S1D). Thus, the BAP complex acts after asymmetric cell division to inhibit the generation of supernumerary type II NBs and prevents tumor formation.

osa Mutations Cause Dedifferentiation of Progenitors

To define the origin of the additional NBs, we analyzed *osa* mutant MARCM clones at various time points. Fifty hours after clone induction, control type II lineages contained a single Dpn$^+$, Ase$^-$ NB (Figure 2A). This was unchanged in *osa* mutant clones (Figure 2A), although Osa protein was undetectable (Figure S2A). In addition, control clones contained two to three Dpn$^-$, Ase$^-$ and three to four Dpn$^-$, Ase$^+$ imINPs, and this number was slightly but significantly increased in *osa* mutant clones (Dpn$^-$, Ase$^-$ imINPs: control 2.62 ± 0.18 SEM [n = 13 clones], and *osa*^{308} 3.5 ± 0.26 SEM [n = 12 clones]; p = 0.01). Seventy-five hours after clone induction, however, *osa* mutant clones contained several Dpn$^+$, Ase$^-$ cells (2.24 ± 0.55 SEM, n = 21 clones) (Figure 2B), although the number of Dpn$^-$, Ase$^-$

(D) Control and *osa* mutant MARCM clones marked by membrane-bound GFP, stained for Dpn and Ase 98 hr after clone induction. Control clone has one Dpn$^+$, Ase$^-$ type II NB (left panel, indicated by an arrow). *osa*^{308} clone contains multiple Dpn$^+$, Ase$^-$ type II NB-like cells (marked with arrows).

(E) As in the control type II NB, pH3$^+$-mitotic NB expressing *osa* shmiR shows asymmetric localization of aPKC (apical marker, yellow arrows) and Mira (basal marker, white arrows).

Scale bars: 10 μm (A and E), 15 μm (D). See also Figure S1.

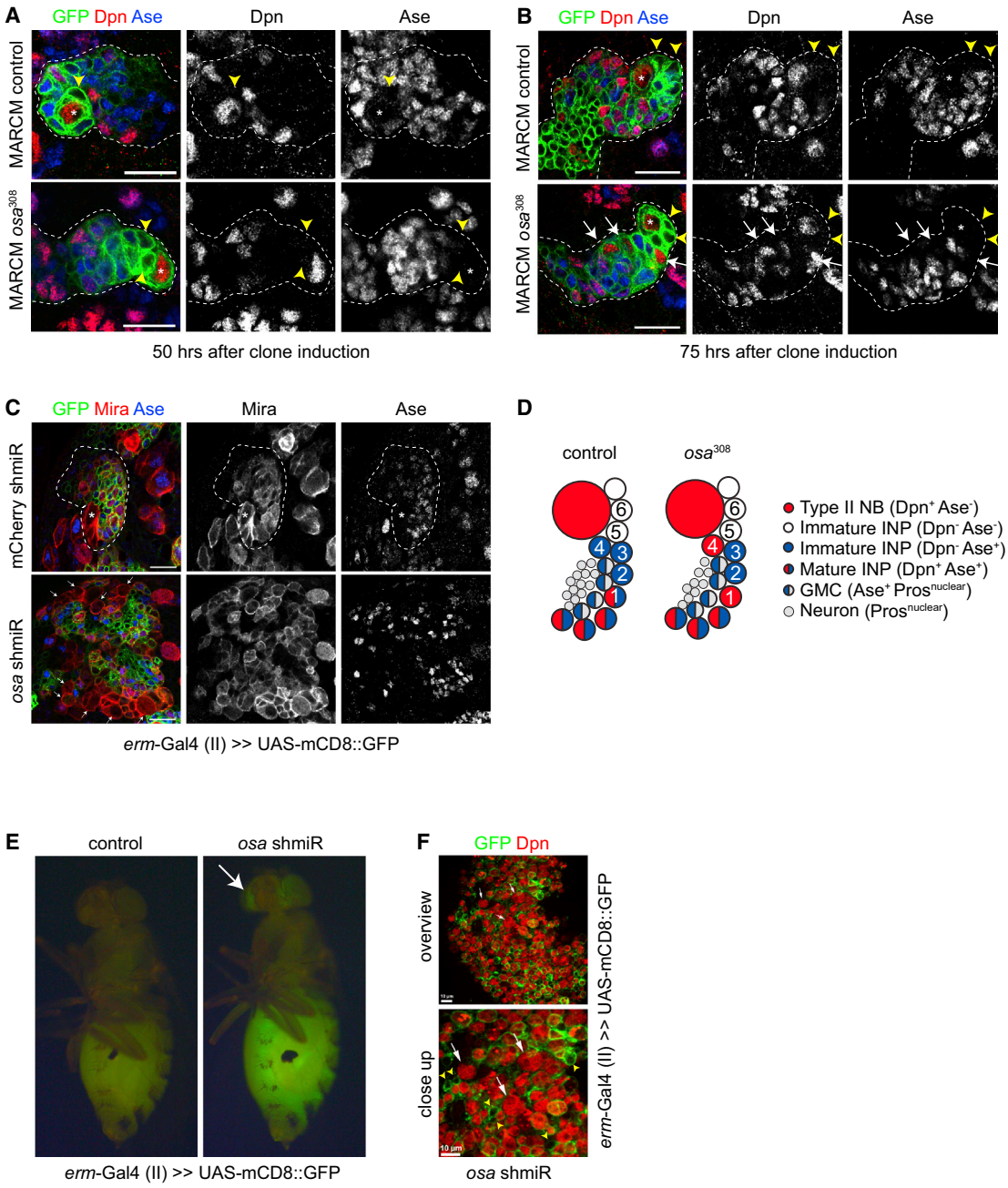

Figure 2. *osa* Mutant Dpn$^-$, Ase$^-$ imINPs Revert to NB-like Cells

(A and B) Control and *osa*^{308} MARCM clones (outlined), stained for Dpn and Ase, analyzed at indicated time points after clone induction.

(A) Fifty hours after clone induction, *osa*^{308} clone has a single Dpn$^+$, Ase$^-$ type II NB (marked with an asterisk), indistinguishable from the control clone. Yellow arrowheads indicate Dpn$^-$, Ase$^-$ imINPs.

(B) Seventy-five hours after clone induction, ectopic Dpn$^+$, Ase$^-$ type II NB-like cells (marked with white arrows) emerge in the *osa*^{308} clone. Most recently born daughter cells (marked with yellow arrowheads) are correctly specified (Dpn$^-$, Ase$^-$). Parental NB is marked with an asterisk.

(C) Close-up images of larval brains expressing *osa* shmiR in Dpn$^-$, Ase$^-$ imINPs by *erm*-GAL4 (II), stained for Mira and Ase, contain supernumerary Mira$^+$, Ase$^-$ cells (white arrows).

(D) Cartoon showing the control and mutant lineage. Numbers indicate birth order.

(E) GFP$^+$ tissue from larval brains expressing *osa* shmiR by *erm*-GAL4 (II) transplanted into the abdomens of host flies causes tumor formation (green abdomen and green spots in the eye [indicated by a white arrow]). GFP levels are low due to loss of GFP expression in revertant cells.

(F) Overview and close-up images of extracted tissue from the transplanted host stained for Dpn. Large Dpn$^+$, GFP$^-$ revertant cells (indicated by white arrows) are neighbored by Dpn$^-$, GFP$^+$ imINPs (indicated by yellow arrowheads).

Scale bars: 15 μm (A, B, and C), 10 μm (F). See also Figure S2 and Movies S1 and S2.

imINPs was no longer significantly different from the control (control 2.64 ± 0.34 SEM [n = 14 clones], and *osa*^{308} 3 ± 0.27 SEM [n = 21 clones]; $p > 0.05$). Similarly, there was no significant difference in the number of mINPs (control 28.57 ± 2.44 SEM [n = 7 clones], and *osa*^{308} 23.75 ± 2.35 SEM [n = 21 clones]; $p > 0.05$). Supernumerary Dpn$^+$, Ase$^-$ cells were several cell diameters away from the primary NB (Figure 2B). Similar observations were made in *snr1* mutant clones (Figure S2B). Because live-imaging experiments indicated that the revertant NBs behave similar to normal NBs in terms of cell-cycle length and lineage (Movies S1 and S2; Figures S2C–S2E), we conclude that the BAP complex is required for stabilizing cell fate, and in its absence, INPs revert to type II NBs.

To determine the precise origin of the reverting cells, we depleted Osa by RNAi in the Dpn$^-$, Ase$^-$ imINPs by *erm*-GAL4 (II) or in the Dpn$^-$, Ase$^+$ imINPs by *erm*-GAL4 (III). *osa* RNAi in the Dpn$^-$, Ase$^-$ imINPs caused formation of supernumerary Mira$^+$, Ase$^-$ cells (Figures 2C and 2D) and transplantable tumors (6 out of 59 flies in *osa* RNAi versus 0 out of 40 flies in control, after 5 weeks) (Figures 2E and 2F), whereas *osa* RNAi in Dpn$^-$, Ase$^+$ imINPs had no effect (Figure S2F). Similar observations were made for *snr1* (Figure S2G). Thus, reverting Dpn$^-$, Ase$^-$ imINPs are the origin of tumor.

Identification of Osa-Regulated Transcriptional Targets

To understand how Osa prevents imINP reversion, we performed transcriptome analysis. We isolated mRNA from FACS-sorted control and Osa-depleted type II lineages of similar cell-type composition (Figures 3A–3C, S3A, and S3B). Deep sequencing identified 49 differentially expressed genes (false discovery rate 0.1; $p < 0.1$; Table S1A). Although Notch activation can also cause lineage reversion (Bowman et al., 2008; Weng et al., 2010; Xiao et al., 2012), we did not identify Notch target genes (Figure S3C), indicating that Osa does not regulate the Notch pathway. Gene Ontology (GO) term analysis of differentially expressed genes revealed a strong enrichment for transcriptional regulators (Table S1B). Because Osa acts in INPs, we FACS sorted type II NBs and INPs/GMCs (Figure S3D) and performed quantitative PCR (qPCR) to find INP-specific targets. As expected, *dpn*, *mira*, *klu*, and *HLHmγ* were expressed in NBs and INPs, whereas *ase* and *erm* were upregulated in INPs (Figure 3D). Of the 13 TFs that were downregulated upon *osa* RNAi (Table S1A, in bold), only *ham*, *oaz*, *opa*, *D*, and *ap* were more than 10-fold upregulated in INPs (Figure 3D). These are likely to be components of a transcriptional program induced by Osa to stabilize the INP fate and prevent INP reversion. RNAi of *oaz*, *opa*, *D*, and *ap* did not cause overproliferation (data not shown), indicating functional redundancy within this program. For *ham*, however, we observed a specific phenotype (see below), and we focused on *ham* for further analysis.

Ham Is a Direct Transcriptional Target of Osa

Antibody staining showed that Ham is neither found in type I nor type II NBs, nor in Ase$^-$ imINPs (Figures 4A and 4B). It is activated with Ase during INP maturation but is absent in *osa* mutant clones (Figure 4B). Chromatin immunoprecipitation (ChIP)-qPCR experiments revealed reproducible binding of Osa upstream of the first and third transcription start sites (TSSs) of the *ham* locus (Figures 4C and S4A) and near the TSSs of the *erm*, *opa*, *oaz*, and *D* loci (Figures S4B and S4C; see below), but not upstream of the *dpn*, *HLHmγ*, or *ase* loci (Figure S4B; data not shown). Analysis of the identified binding sites revealed a GA-rich motif that is enriched in potential Osa targets (see Extended Experimental Procedures; Figure S4D). Although Osa is ubiquitously expressed (Figure 4D), it does not bind to the identified target loci in type II NBs because target binding was reduced to background levels in *brat* mutants where tumors consisting entirely of type II NBs are formed (Figures 4E, S4E, and S4F). Thus, our results indicate that the BAP complex is recruited to specific target loci in INPs where it activates a transcriptional program that prevents reversion to NBs when expression of self-renewal genes is reinitiated.

Ham Limits Proliferation in INPs

To test whether the upregulation of Ham is an essential component of the Osa-induced transcriptional program, we performed rescue experiments (Figures S5A–S5D′). Indeed, tumor formation upon *osa* RNAi was completely prevented upon coexpression of Ham (Figures S5C–S5C′). Thus, upregulation of Ham is sufficient to prevent tumorigenesis in *osa* mutants.

What could be the function of Ham in type II lineages? Unlike its mammalian homologs, Ham does not regulate global heterochromatin formation because the levels of H3K9me1 are not changed in mutant clones (Figure S5E) (Pinheiro et al., 2012). Instead, Ham limits proliferation in INPs because the induction of *ham* RNAi by *erm*-GAL4 resulted in the formation of additional Mira$^+$, Ase$^+$ cells (Figures 5A and S5F). Upon *ham* RNAi, both the numbers of mINPs and GMCs were increased (Figures 5B and 5C), and 2.3-fold more pH3$^+$-mitotic INPs were detected. Similar effects were found in *ham*^{1} mutant clones (mINPs: control 32.33 ± 1.76 SEM [n = 9 clones], and *ham*^{1} 49.11 ± 3.65 SEM [n = 9 clones]; Figures 5D and 5E), and neither aPKC nor Mira localization was affected (Figure 5F). Importantly, however, *ham* mutant INPs did not revert to NBs (Figure 5D), and *ham* RNAi did not result in tumor formation upon transplantation (0 out of 58 flies upon transplantation of *ham* RNAi-expressing tissue, after 5 weeks), indicating partial redundancy with other Osa downstream targets.

To determine the origin of the supernumerary cells, we analyzed the division patterns of INPs and their daughters by live imaging in culture. Control INPs and INPs expressing *ham* RNAi divided at the same rate (Figure S6A), reproducibly generating a GMC that divides once more into two differentiating neurons (Figures S6B–S6K; Movies S3 and S4) (control, n = 24 INPs, *ham* RNAi n = 29 INPs followed for three to four divisions). Thus, excessive INPs upon Ham loss are not due to altered division rates, symmetric INP divisions, or GMC-to-INP reversion. In addition, TUNEL staining revealed almost no apoptotic wild-type (WT) INPs (Figure S6L), excluding reduced cell death as a potential mechanism. Taken together, these experiments suggest that INPs remain proliferative for an extended period in *ham* mutants. Thus, we conclude that Ham is required to restrict the number of asymmetric divisions in the TA population of type II lineages.

To test whether Ham is also sufficient to limit self-renewal, we ectopically expressed the protein in NBs. All except one to two

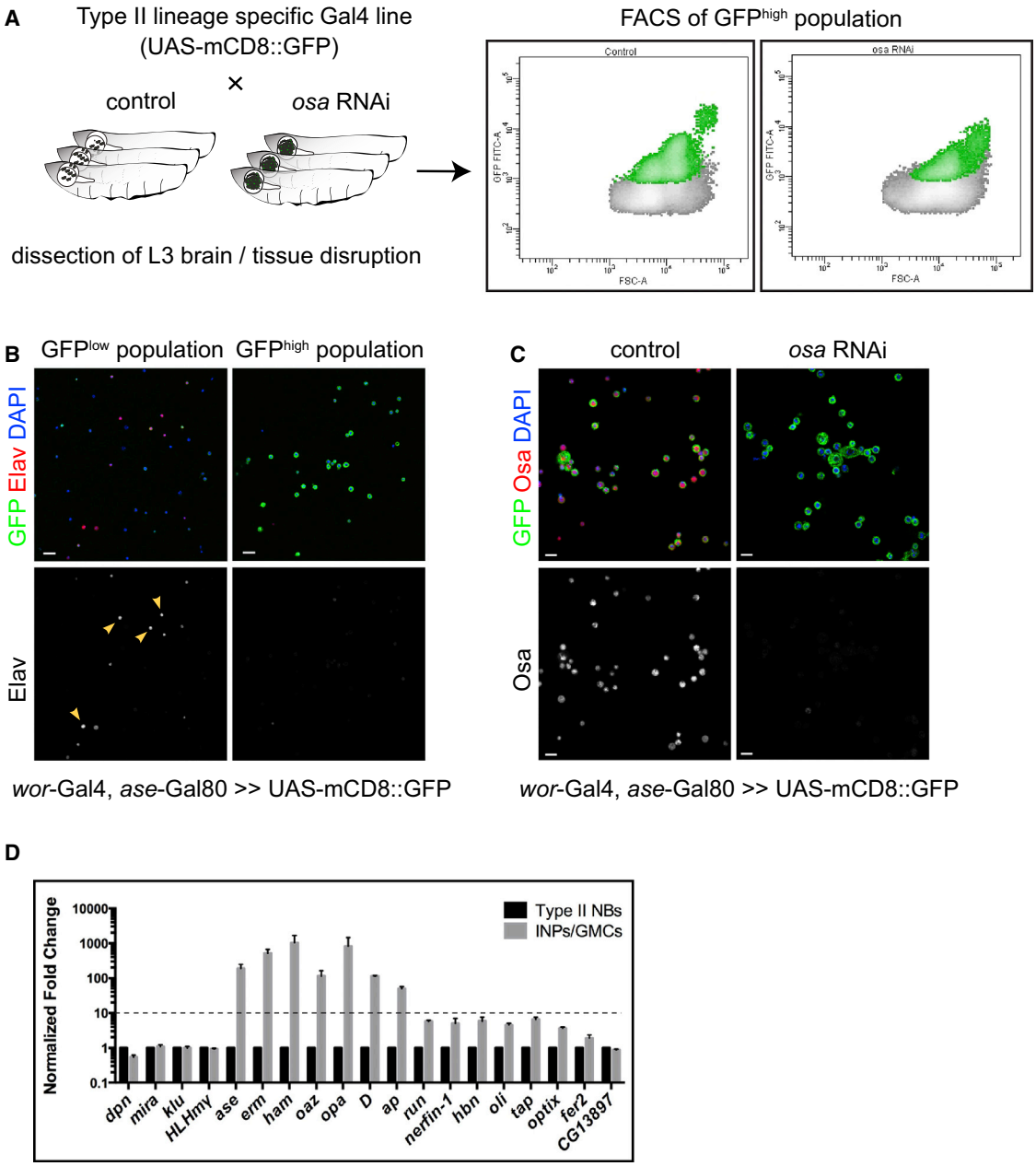

Figure 3. FACS of Type II Lineages Expressing *osa* RNAi

(A) Cartoon illustrating the FACS of control and *osa* RNAi-expressing type II lineages. Cells were FACS sorted into GFP^{low} (gray) and GFP^{high} (green) populations. Size (x axis) versus GFP intensity (y axis) plot shows the shift in the cell size and GFP levels upon *osa* RNAi.

(B) GFP^{high} population is devoid of Elav^{+} neurons (indicated by arrowheads).

(C) Osa staining of FACS-sorted control and *osa* RNAi-expressing GFP^{high} populations. Osa is efficiently depleted in FACS-sorted cells.

(D) qPCR analysis of candidate target gene expression levels in FACS-sorted control type II NBs versus INPs/GMCs. Error bars, SEM.

Scale bars: 20 μm (B), 10 μm (C). See also Figure S3 and Table S1.

type II lineages per brain lobe were lost upon Ham overexpression (Figures S5D–S5D′). This is not due to apoptosis because the phenotype cannot be rescued by the apoptosis inhibitor *p35* (zero type II NBs detected, n = 7 brains) (Figure S6M). Twenty-four hours after the induction of Ham expression by *PntP1*-GAL4 (McGuire et al., 2004; Zhu et al., 2011), the average NB diameter decreased by 22% (control 11.5 ± 0.5 μm SEM [n = 10 type II NBs], and UAS-*ham* 8.9 ± 0.2 μm SEM [n = 10 type II NBs]; $p < 0.001$). In addition, 64% of type II NBs activated Ase (n = 14 type II NBs), and NBs started to downregulate the *PntP1*-GAL4 driver (Figure 6A), indicating loss of NB identity. When expressed in type I NBs, Ham resulted in 80% NB loss

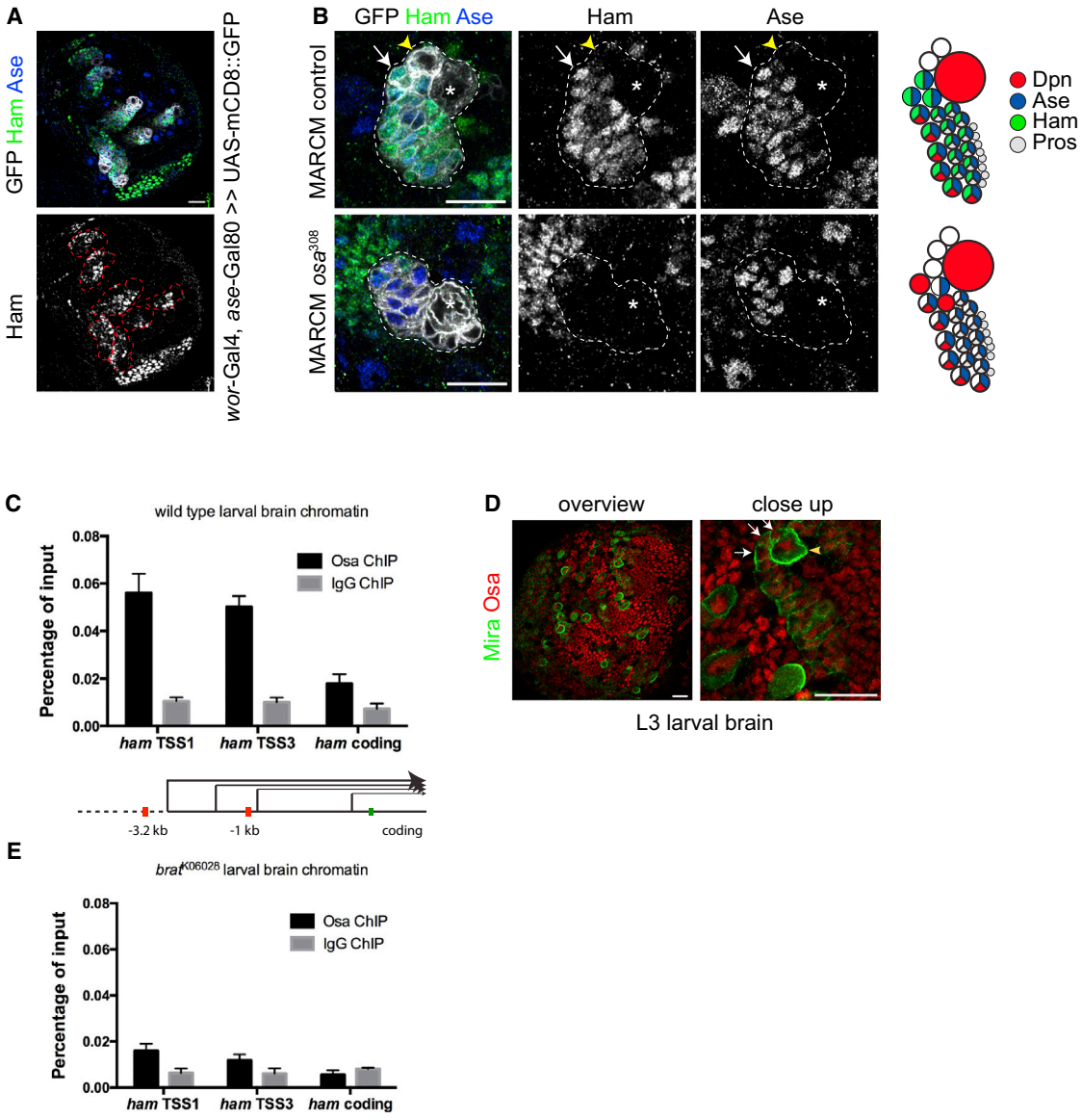

Figure 4. Ham Is Activated Directly by Osa in the INPs

(A) Ham expression in the central brain is limited to the type II lineages. Overview image of a brain lobe stained for Ham and Ase is shown. Type II lineages are outlined by red dashed lines.

(B) Control and *osa*^{308} MARCM clones stained for Ham and Ase 75 hr after clone induction. Control clones contain a Ham^{-} NB (indicated by asterisks) and imINPs (marked with yellow arrowheads). Ham and Ase are coexpressed during INP maturation (marked with arrows). *osa*^{308} clones have Ase^{+} INPs but lack Ham^{+} cells. Schematic of various markers in control versus *osa*^{308} clones is shown to the right.

(C) ChIP-qPCR analysis at *ham* locus in WT larval brain tissue for Osa and control IgG. ChIP signals are represented as the percentage of input chromatin. Distances from the closest TSS are indicated in kilobases in the scheme of *ham* locus below. A region in the *ham*-coding sequence was selected as negative control.

(D) Osa is ubiquitously expressed in the larval brain. Type II NB (marked with a yellow arrowhead) and most recently born INPs (marked with white arrows) have similar Osa levels.

(E) ChIP-qPCR analysis at *ham* locus in *brat* mutant larval brain tissue for Osa and control IgG. ChIP signals are represented as the percentage of input chromatin.

Error bars, SEM in (C) and (E). Scale bars, 20 μm (A and D) and 15 μm (B). See also Figure S4.

(Figures 6B and 6C). The remaining NBs had less progeny (Figure 6B), were smaller (Figure 6D), and often showed nuclear Pros (11%, n = 5 brains, Figure 6E). In culture, Ham-expressing type I NBs generated fewer progeny due to increased cell-cycle times (Figures S6N–S6P; Movies S5 and S6). Thus, Ham is a potent inhibitor of self-renewing divisions and cellular growth in *Drosophila* neural stem cells. We propose that Ham is upregulated by Osa in INPs to limit their self-renewal capacity, so that they divide only a limited number of times, a feature that distinguishes them from NBs.

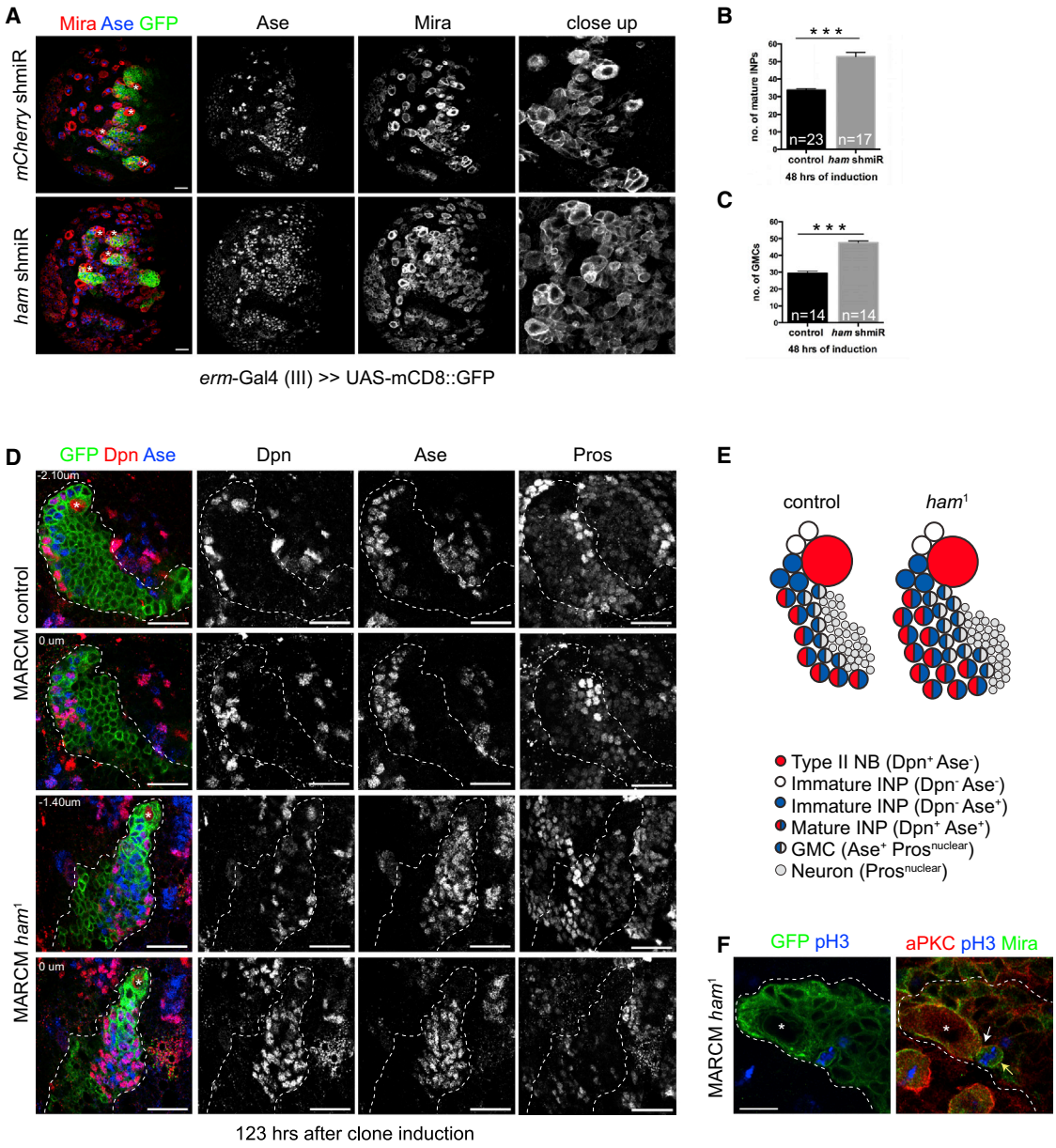

Figure 5. Ham Is Required in the INPs to Limit Self-Renewal

(A) *ham* shmiR expression in larval brains by *erm*-GAL4 (III) increases the number of Mira$^+$, Ase$^+$ cells. Type II NBs are indicated by asterisks.

(B and C) Quantification of mINP (Dpn$^+$, Ase$^+$) and GMC (Ase$^+$, Pros$^+$) numbers 48 hr after *ham* shmiR induction by *insc*-GAL4; *tub*-Gal80^{ts}. Error bars, SEM. n, number of type II lineages analyzed.

(D) Control and *ham*^{1} MARCM clones, stained for Dpn, Ase, and Pros 123 hr after clone induction. Two separate z stacks are shown. *ham*^{1} clones have an increased number of Ase$^+$ cells.

(E) Cartoon summarizing *ham*^{1} phenotype.

(F) aPKC and Mira segregate normally in *ham* mutant INPs. Dashed lines outline clone; asterisks mark type II NB. Arrows mark aPKC and Mira crescent.

Scale bars: 20 μm (A and D), 10 μm (F). ***p < 0.001, Student's t test. See also Figures S5 and S6 and Movies S3 and S4.

Osa and Ham Are Required for Temporal Patterning in INPs

Besides Ham, our search for Osa targets in INPs identified the Sox domain TF D (Table S1A) (Russell et al., 1996). In mammals, Sox factors play important roles in multiple stem cell lineages (Sarkar and Hochedlinger, 2013). In *Drosophila*, D is part of a series of TFs (D, Grh, and Ey) that confer temporal identity to INPs and ensure timely cell-cycle exit (Bayraktar and Doe, 2013). Indeed, antibody staining confirmed that *osa* mutant clones failed to activate *D* expression 72 hr after clone induction (Figure 7A). As for Ham, ChIP-qPCR experiments demonstrated that Osa directly binds to the *D* locus upstream of the second

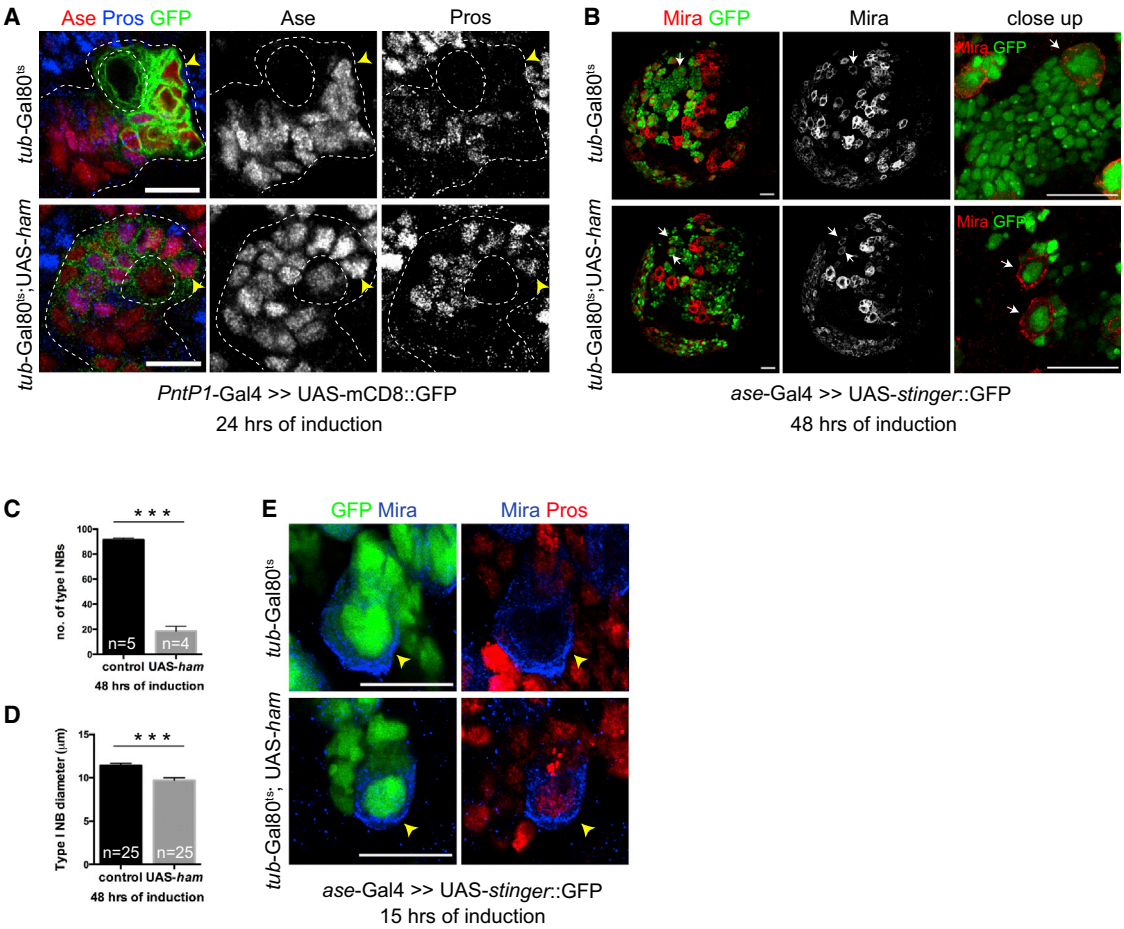

Figure 6. Ham Overexpression Is Sufficient to Limit NB Self-Renewal

(A) Expression of Ham in type II NBs for 24 hr by *PntP1*-GAL4 causes premature differentiation. Control type II NB is Ase$^-$ (upper panel). Ham expressing type II NB is Ase$^+$ (lower panel). Unlike WT NB, Ham expressing NB is surrounded by Pros$^+$ progeny (yellow arrowheads).

(B) Larval brains expressing Ham in the type I NBs for 48 hr by *ase*-GAL4 have reduced numbers of type I NBs seen as a reduction in the number of GFP$^+$ progeny and Mira$^+$ cells.

(C) Graph showing the decrease in the number of type I NBs upon Ham expression for 48 hr. n, number of brains.

(D) Graph showing the decrease in the NB diameter upon Ham expression for 48 hr. n, number of type I NBs.

(E) Type I NBs (marked by yellow arrowheads) expressing Ham for 15 hr show nuclear Pros staining, indicating premature differentiation.

Scale bars: 10 μm (A), 20 μm (B), and 15 μm (E). Error bars, SEM in (C) and (D). ***$p < 0.001$, Student's t test. See also Figures S5 and S6 and Movies S5 and S6.

TSS (Figure 7B). Thus, in addition to upregulating Ham, Osa also initiates temporal patterning in INPs.

The functional connections between Osa, D and Ham prompted us to test whether Ham could actually control the number of INP divisions by influencing temporal patterning. In contrast to *osa* mutants, INPs depleted for Ham successfully activated D and Grh (Figures 7C and S7A). Unlike in control, however, expression of Grh was not repressed in middle-aged INPs upon *ham* RNAi (Figures 7C and S7B). As a consequence, the percentage of Ey$^+$ INPs was significantly reduced (Figure S7C), although Ey expression was not completely blocked (Figure S7D). Thus, INPs require Ham to transit from the middle-aged Grh$^+$, Ey$^+$ to the old Grh$^-$, Ey$^+$ stage (Figure 7D). Consistent with this, Toy$^+$ neurons generated from those "old" INPs were almost entirely missing in Ham-depleted clones (Figures S7E and S7F) (Bayraktar and Doe, 2013). In addition, the lifespan of INPs was severely extended upon *ham* RNAi. Type II NBs disappear ~0–16 hr after larvae undergo pupariation (after puparium formation [APF]) at 29°C, and after this stage, the number of INPs is gradually reduced as they exit proliferation (Homem and Knoblich, 2012; Maurange et al., 2008; Truman and Bate, 1988) (data not shown). WT pupal brains contained few Grh$^+$ INPs 25 hr APF (Figure 7E) and none 50 hr APF (Figure 7F). Upon *ham* RNAi, however, pupal brains contained numerous Grh$^+$ INPs 25 hr APF (Figure 7E), some of which even perdured to 50 hr APF (Figure 7F). Thus, the function of Ham is required in INPs to complete their temporal patterning program and for timely cell-cycle exit.

Taken together, our data indicate that SWI/SNF activates a "transit-amplifying" program in imINPs that induces temporal patterning, restricts self-renewal capacity, and prevents reversion to NBs (Figures 7G and 7H). Ham is a key component of

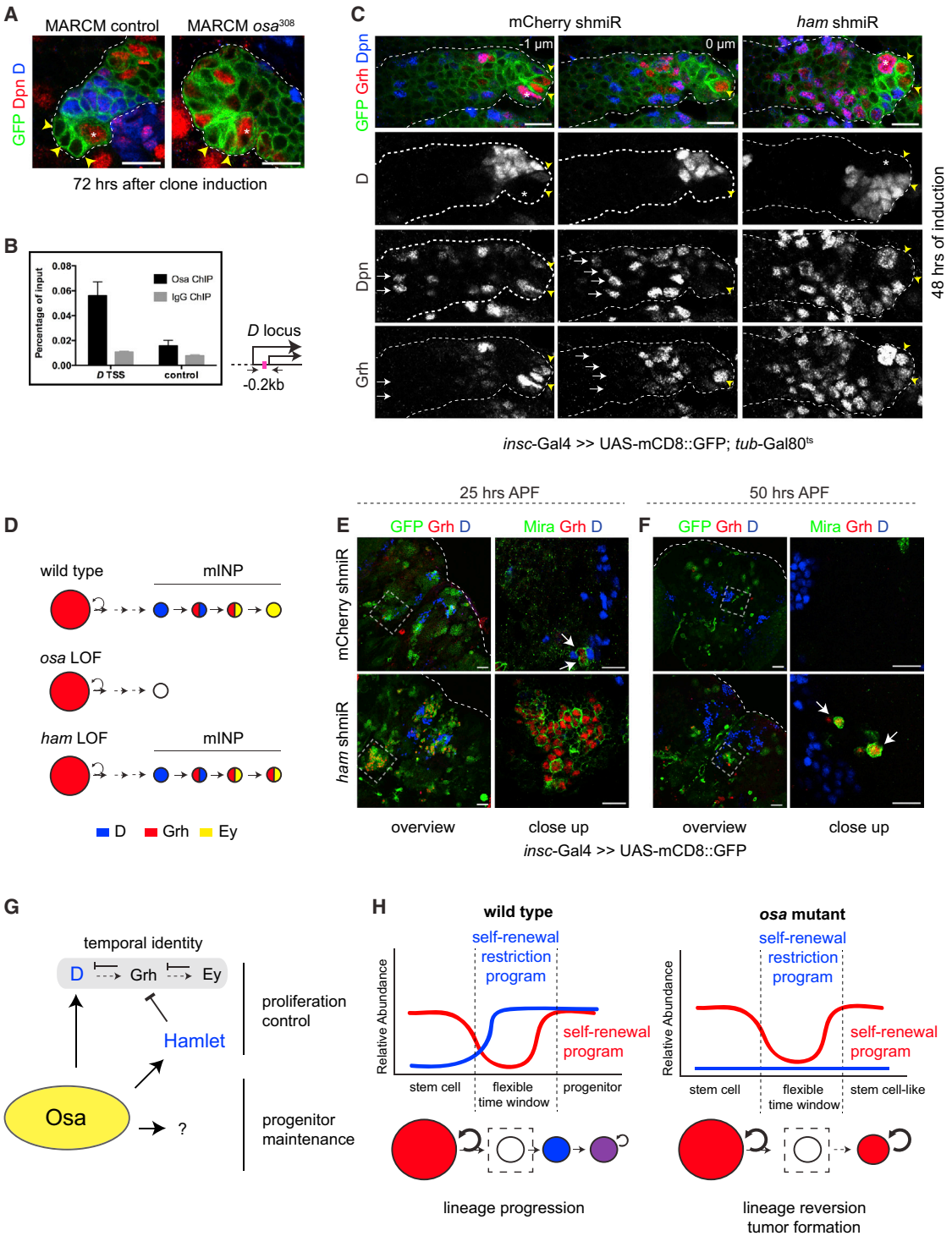

Figure 7. Osa and Ham Are Required for the Temporal Patterning of INPs

(A) Control and *osa*^{308} MARCM clones stained for D and Dpn 72 hr after clone induction. *osa* mutant INPs fail to activate D.

(B) ChIP-qPCR analysis at *D* locus for Osa and control IgG. ChIP signals are represented as the percentage of input chromatin. Distance from the closest TSS is indicated in kilobases in the scheme of *D* locus. Error bars, SEM.

(C) Close-up images of larval brains expressing *ham* shmiR for 48 hr by *insc*-GAL4; *tub*-Gal80^{ts}, stained for D, Grh, and Dpn. In the control type II lineage (dorsomedial 2) (two separate z stacks are shown), type II NB (indicated by an asterisk) and imINPs (yellow arrowheads) are Grh^{+}. Grh is initially downregulated during INP maturation, and D is upregulated. Middle-aged INPs resume Grh expression. As INPs transit from middle aged to old, Grh is downregulated (Dpn^{+} cells marked with white arrows). Upon *ham* RNAi, middle-aged INPs fail to downregulate Grh.

(legend continued on next page)

this program that limits the number of ensuing self-renewal divisions by ensuring the progression of temporal patterning initiated by the SWI/SNF complex.

DISCUSSION

Our data reveal an essential function for the chromatin-remodeling SWI/SNF complex in ensuring lineage progression in stem cell lineages. When neural stem cells/NBs progress toward the TA/INP fate, the SWI/SNF complex activates a transcriptional program that limits self-renewal and initiates a temporal TF cascade to confer temporal identity. Failure to do so results in lineage reversion and tumor formation. We identify the temporal TF D and the Prdm protein Ham as direct SWI/SNF targets and show that induction of Ham limits the number of TA divisions by ensuring the progression of temporal patterning (Figure 7G). Members of the SWI/SNF complex, particularly the Osa homologs ARID1A and ARID1B, are among the most frequently mutated genes in human cancer, and our findings provide a potential mechanism for their tumor-suppressing activity.

We propose a model where two distinct transcriptional programs act in concert to ensure directionality in *Drosophila* neural stem cell lineages (Figure 7H). In type II NBs, a "self-renewal" program comprising the TFs Dpn, Klu, and HLHmγ allows long-term self-renewal (Berger et al., 2012; San-Juán and Baonza, 2011; Song and Lu, 2011; Xiao et al., 2012; Zacharioudaki et al., 2012; Zhu et al., 2011). Upon asymmetric division, Numb and Brat terminate this program in one of the two daughter cells, which therefore progresses toward the imINP stage. As INPs undergo maturation, Brat and Numb disappear, allowing the program to reinitiate and self-renewal to resume. Our data indicate that Osa activates a second "self-renewal restriction" program before this reinitiation occurs to ensure that INPs, unlike NBs, differentiate after around five rounds of asymmetric cell division. In *osa* mutants, the restriction program is not activated. The self-renewal program, however, is unaffected, and therefore, INPs regain NB-like properties resulting in unlimited self-renewal and brain tumor formation (Figure 7H).

Why does Osa not activate the self-renewal restriction program in NBs? In mammalian neural stem cells, a subunit switch in the SWI/SNF complex is thought to trigger the switch from self-renewal to differentiation (Lessard et al., 2007; Wu et al., 2007, 2009; Yoo and Crabtree, 2009), but we could not detect a similar switch in the *Drosophila* larval brain (data not shown). More likely, Dpn, Klu, and HLHmγ prevent Osa binding in NBs, for example by competing with SWI/SNF for binding sites. In fact, all three factors can act as transcriptional repressors (Bier et al., 1992; Jennings et al., 1994; Klein and Campos-Ortega, 1997), and *opa* (one of the SWI/SNF targets we identified) is actually also a direct Dpn target in the embryonic CNS (Southall and Brand, 2009).

Our results suggest a tight functional connection between the SWI/SNF complex and the temporal TF cascade that confers temporal identity to INPs. SWI/SNF directly induces transcription of D, the first member of this cascade. In addition, it induces Ham, a chromatin regulator that can limit self-renewal capacity in INPs but also when ectopically expressed in NBs. In INPs, Ham is specifically required for the transition from Grh^+, Ey^+ middle-aged INPs to Grh^-, Ey^+ old INPs. Because transition to the terminal transcriptional state is important for timely cell-cycle exit in mINPs (Bayraktar and Doe, 2013), this explains the overproliferation phenotype observed in *ham* mutants.

How could Ham mediate temporal progression of INPs? It has been previously shown that recruitment of the earliest component of the NB "transcriptional clock" to the nuclear periphery permanently silences its expression and limits NB competence (Kohwi et al., 2013). Evi1 and Prdm16, the mammalian homologs of Ham, have been postulated to initiate heterochromatin formation by methylating H3K9 (Pinheiro et al., 2012). Because H3K9 methylation is crucial for recruiting gene loci to the nuclear periphery, it is interesting to speculate that Ham acts in INPs by driving the transition to the next transcriptional state and, ultimately, to differentiation (Gonzalez, 2013; Towbin et al., 2012; Yuzyuk et al., 2009).

Mutations in the mammalian SWI/SNF complex subunits are potential drivers of tumorigenesis in a wide variety of tissues including the brain (Kadoch et al., 2013; Shain and Pollack, 2013; Wilson and Roberts, 2011). The Brm homolog SMARCA4 and the Osa homologs ARID1A and ARID1B are among the chromatin modifiers that are recurrently mutated in medulloblastoma, the most common malignant childhood brain tumor (Northcott et al., 2012; Parsons et al., 2011). Identifying the cell of origin in brain tumors is crucial in designing effective therapeutic strategies (Liu and Zong, 2012). Stem cells could acquire oncogenic mutations that initiate tumor formation (Alcantara Llaguno et al., 2009). On the other hand, tumors could also originate from more restricted progenitors that inherit these mutations and become malignant (Liu et al., 2011; Schüller et al., 2008; Yang et al., 2008). Our study offers an alternative explanation: provided that the function of SWI/SNF is conserved in humans, mutations occurring in restricted progenitors could affect lineage progression causing progenitors to revert into stem cells. In this case, the cell of origin would be a progenitor despite the fact that tumors are made up of stem cells. In fact, this possibility has been proposed for other tumor suppressors (Schwitalla et al., 2013) and

(D) Cartoon summarizing the defects in INP temporal patterning upon *ham* and *osa* loss of function (LOF).
(E and F) Overview and close-up images of pupal brains expressing *ham* shmiR by *insc*-GAL4 stained for Mira, Grh, and D (E) 25 hr or (F) 50 hr APF at 29°C.
(E) Control brain contains few $Mira^+$, Grh^+ INPs (indicated by white arrows in close-up images), whereas *ham* shmiR-expressing brain contains several.
(F) Fifty hours APF (at 29°C), no $Mira^+$, Grh^+ INPs are detected in the control brain. *ham* shmiR-expressing brain contains few $Mira^+$, Grh^+ INPs (indicated by white arrows).
(G and H) Graphical model.
(G) Osa directly activates D and Ham to ensure proliferation control in progenitors.
(H) Although the self-renewal program is not affected in *osa* mutants, the self-renewal restriction program fails to turn on, and progenitors revert to NB-like cells.
Scale bars, 10 μm (A and C), 30 μm (overview images), and 15 μm (close-up images in E and F). See also Figure S7.

could be tested rigorously for SWI/SNF mutations given the recent significant advances in cell lineage tracing in tumors (Chen et al., 2012; Driessens et al., 2012; Schepers et al., 2012).

EXPERIMENTAL PROCEDURES

Drosophila Strains and Clonal Analysis

Drosophila stocks used in this study were *brm* RNAi (transformant ID [TID] 37720 and 37721; Vienna Drosophila RNAi Center [VDRC]); *mor* RNAi (TID 6969 and 110712; VDRC); *osa* RNAi (TID 7810; VDRC); *ham* shmiR (BL32470); *osa* shmiR (generated in this study); *snr1* RNAi (TID 108599; VDRC); *snr1* shmiR (BL32372); *mCherry* shmiR (BL35785); $brat^{K06028}$ (Arama et al., 2000); UAS-*ham* (Moore et al., 2002); UAS-p35; and mγ-GFP (Almeida and Bray, 2005). Mutant fly strains used for clonal analysis were ham^{1}, FRT40A (Moore et al., 2002), FRT40A; *ham* shmiR, FRT82B, osa^{308} (Treisman et al., 1997) (BL5949), and FRT82B, $snr1^{R3}$ (Zeng et al., 2013). GAL4 driver lines used were UAS-*dcr2*; *insc*-GAL4, UAS-mCD8-GFP; *tub*-$Gal80^{ts}$ (Neumüller et al., 2011), *ase*-GAL4, UAS-*stinger*-GFP (Zhu et al., 2006), UAS-mCD8-GFP;;*PntP1*-GAL4 (Zhu et al., 2011), *erm*-GAL4 (II); UAS-mCD8-GFP (Xiao et al., 2012), UAS-mCD8-GFP; *erm*-GAL4 (III) (Pfeiffer et al., 2008; Weng et al., 2010), UAS-*dcr2*; *wor*-GAL4, *ase*-Gal80; UAS-mCD8-GFP (Neumüller et al., 2011), UAS-*dcr2*; *wor*-GAL4, *ase*-Gal80;UAS-*stinger*-RFP (Homem et al., 2013). Clones of NBs homozygous for osa^{308}, $snr1^{R3}$, or ham^{1} were generated by Flippase (FLP)/FLP recombination target (FRT)-mediated mitotic recombination, using the *elav*-GAL4 (C155) (Lee and Luo, 1999). Larvae were heat shocked for 1 hr at 38°C and dissected as wandering third-instar larvae. RNAi crosses were set up and reared at 29°C, and wandering third-instar larvae were dissected 5 days after. For analysis of INP perdurance, white prepupae were collected and staged at 29°C for 25 or 50 hr.

Antibodies

Antibodies generated in this study were guinea pig anti-Osa (maltose-binding protein [MBP] fusion of aa 2,123–2,717, affinity purified IgGs, 7.5 μg/ChIP); rabbit anti-Ham (against the peptide DAFFKDRAQAEHILQEWVRRREPVC, affinity purified, 1:50); guinea pig anti-Dpn (against full-length MBP fusion protein, serum, 1:1,000); rat anti-Ase (Bhalerao et al., 2005); and rabbit anti-Pros (serum, 1:1,000; Vaessin et al., 1991). Other antibodies used were mouse anti-Osa (Developmental Studies Hybridoma Bank [DSHB]); guinea pig anti-Ase (1:100; Bhalerao et al., 2005); rabbit anti-Mira (1:100; Betschinger et al., 2006); guinea pig anti-Mira (1:100); chicken GFP (1:500; Abcam); mouse anti-Pros (1:100; DSHB); mouse anti-pH3 (1:1,000; Cell Signaling Technology); rat anti-Elav (1:100 7E8A10; DSHB); rabbit anti-aPKC (1:500; Santa Cruz Biotechnology); rabbit anti-Numb (1:100; Schober et al., 1999); rabbit anti-Brat (1:100; Betschinger et al., 2006); rat anti-Grh (1:1,000; Baumgardt et al., 2009); rabbit anti-D (1:1,000; Ma et al., 1998); mouse anti-Ey (1:10; DSHB); guinea pig anti-Toy (gift from U. Walldorf), rabbit anti-H3K9me1 (9045; Abcam); Alexa Fluor 488 phalloidin (Invitrogen); and normal guinea pig IgG (Santa Cruz Biotechnology). In situ cell death detection kit (TMR red by Roche; 12156792910) was used for TUNEL staining.

Cell Dissociation, FACS, Sample Preparation, and RNA Sequencing

Cell dissociation, FACS, and bioinformatic analysis were done as previously described with minor modifications (Berger et al., 2012; Harzer et al., 2013). UAS-*dcr2*; *wor*-GAL4, *ase*-Gal80; UAS-mCD8-GFP line was used to induce the expression of membrane-bound GFP and *osa* RNAi. Decreasing levels of GFP were observed in neurons due to lack of driver expression in differentiated cells. Because tumors arising from *osa* RNAi are enriched for type II NBs and INPs and contain less neurons, GFP^{high} and GFP^{low} populations were separated to exclude neurons. A total of 200–300 larval brains were dissected to obtain sufficient WT type II NBs and INPs per replicate of the qPCR experiment. Seventy-six-base pair Illumina paired-end sequencing of Poly-A-mRNA libraries was performed on GAIIx. The experiment lacked biological replicates due to difficulties in getting sufficient material to prepare the sequencing library. For the analysis, DESeq was instructed to ignore the condition labels and estimate the variance by treating all the samples as if they were replicates of the same condition (method = "blind") (Anders and Huber, 2010).

ChIP

ChIP experiments were performed as described before by Lee et al. (2006) and Richter et al. (2011) with minor modifications. See Extended Experimental Procedures for details and qPCR primer sequences.

qPCR Analysis of FACS-Sorted Cells

First-strand cDNA was generated using random primers on TRIzol-extracted total FACS-sorted cell RNA. qPCR was done using Bio-Rad IQ SYBR Green Supermix on a Bio-Rad CFX96 cycler. Expression of each gene was normalized to RpS8, and relative levels were calculated using the $2^{-\Delta\Delta C_T}$ method (Livak and Schmittgen, 2001). See Extended Experimental Procedures for qPCR primer sequences.

ACCESSION NUMBERS

The Gene Expression Omnibus accession number for the RNA-sequencing data reported in this paper is GSE48242.

SUPPLEMENTAL INFORMATION

Supplemental Information includes Extended Experimental Procedures, seven figures, six movies, and one table and can be found with this article online at http://dx.doi.org/10.1016/j.cell.2014.01.053.

ACKNOWLEDGMENTS

We thank I. Reichardt, M. Lancaster, and H. Harzer for critical comments on the manuscript; A.W. Moore, C.Y. Lee, Y.N. Jan, S. Thor, S.X. Hou, U. Walldorf, the Bloomington *Drosophila* Stock Center, the Vienna *Drosophila* RNAi Center, the Developmental Studies Hybridoma Bank, and TriP at Harvard Medical School (NIH/NIGMS R01-GM084947) for fly stocks and reagents; F. Mauri for the help with generating Dpn antibody; H. Harzer for generating the rabbit Pros antibody; J. Steinmann for the help with the shmiR design; M. Madalinski for peptide synthesis and affinity purification; G. Schmauss and T. Lendl for FACS support; P. Pasierbek for bio-optics support; and CSF NGS unit for next-generation sequencing. Work in J.A.K.'s lab is supported by the Austrian Academy of Sciences, the Austrian Science Fund (FWF, grants I_552-B19, I_1281_B19, and Z_153_B09), and an advanced grant of the European Research Council.

Received: June 21, 2013
Revised: November 11, 2013
Accepted: January 16, 2014
Published: March 13, 2014

REFERENCES

Alcantara Llaguno, S., Chen, J., Kwon, C.H., Jackson, E.L., Li, Y., Burns, D.K., Alvarez-Buylla, A., and Parada, L.F. (2009). Malignant astrocytomas originate from neural stem/progenitor cells in a somatic tumor suppressor mouse model. Cancer Cell *15*, 45–56.

Almeida, M.S., and Bray, S.J. (2005). Regulation of post-embryonic neuroblasts by *Drosophila* Grainyhead. Mech. Dev. *122*, 1282–1293.

Anders, S., and Huber, W. (2010). Differential expression analysis for sequence count data. Genome Biol. *11*, R106.

Arama, E., Dickman, D., Kimchie, Z., Shearn, A., and Lev, Z. (2000). Mutations in the beta-propeller domain of the *Drosophila* brain tumor (brat) protein induce neoplasm in the larval brain. Oncogene *19*, 3706–3716.

Baumgardt, M., Karlsson, D., Terriente, J., Díaz-Benjumea, F.J., and Thor, S. (2009). Neuronal subtype specification within a lineage by opposing temporal feed-forward loops. Cell *139*, 969–982.

Bayraktar, O.A., and Doe, C.Q. (2013). Combinatorial temporal patterning in progenitors expands neural diversity. Nature *498*, 449–455.

Bello, B.C., Izergina, N., Caussinus, E., and Reichert, H. (2008). Amplification of neural stem cell proliferation by intermediate progenitor cells in *Drosophila* brain development. Neural Dev. *3*, 5.

Berger, C., Harzer, H., Burkard, T.R., Steinmann, J., van der Horst, S., Laurenson, A.S., Novatchkova, M., Reichert, H., and Knoblich, J.A. (2012). FACS purification and transcriptome analysis of *drosophila* neural stem cells reveals a role for Klumpfuss in self-renewal. Cell Rep. *2*, 407–418.

Betschinger, J., Mechtler, K., and Knoblich, J.A. (2006). Asymmetric segregation of the tumor suppressor brat regulates self-renewal in *Drosophila* neural stem cells. Cell *124*, 1241–1253.

Bhalerao, S., Berdnik, D., Török, T., and Knoblich, J.A. (2005). Localization-dependent and -independent roles of numb contribute to cell-fate specification in *Drosophila*. Curr. Biol. *15*, 1583–1590.

Bier, E., Vaessin, H., Younger-Shepherd, S., Jan, L.Y., and Jan, Y.N. (1992). deadpan, an essential pan-neural gene in *Drosophila*, encodes a helix-loop-helix protein similar to the hairy gene product. Genes Dev. *6*, 2137–2151.

Boone, J.Q., and Doe, C.Q. (2008). Identification of *Drosophila* type II neuroblast lineages containing transit amplifying ganglion mother cells. Dev. Neurobiol. *68*, 1185–1195.

Bowman, S.K., Rolland, V., Betschinger, J., Kinsey, K.A., Emery, G., and Knoblich, J.A. (2008). The tumor suppressors Brat and Numb regulate transit-amplifying neuroblast lineages in *Drosophila*. Dev. Cell *14*, 535–546.

Brand, A.H., and Livesey, F.J. (2011). Neural stem cell biology in vertebrates and invertebrates: more alike than different? Neuron *70*, 719–729.

Caussinus, E., and Gonzalez, C. (2005). Induction of tumor growth by altered stem-cell asymmetric division in *Drosophila melanogaster*. Nat. Genet. *37*, 1125–1129.

Chen, J., Li, Y., Yu, T.S., McKay, R.M., Burns, D.K., Kernie, S.G., and Parada, L.F. (2012). A restricted cell population propagates glioblastoma growth after chemotherapy. Nature *488*, 522–526.

Clarke, M.F., and Fuller, M. (2006). Stem cells and cancer: two faces of eve. Cell *124*, 1111–1115.

Collins, R.T., Furukawa, T., Tanese, N., and Treisman, J.E. (1999). Osa associates with the Brahma chromatin remodeling complex and promotes the activation of some target genes. EMBO J. *18*, 7029–7040.

Crosby, M.A., Miller, C., Alon, T., Watson, K.L., Verrijzer, C.P., Goldman-Levi, R., and Zak, N.B. (1999). The trithorax group gene moira encodes a brahma-associated putative chromatin-remodeling factor in *Drosophila melanogaster*. Mol. Cell. Biol. *19*, 1159–1170.

de la Serna, I.L., Ohkawa, Y., and Imbalzano, A.N. (2006). Chromatin remodelling in mammalian differentiation: lessons from ATP-dependent remodellers. Nat. Rev. Genet. *7*, 461–473.

Dingwall, A.K., Beek, S.J., McCallum, C.M., Tamkun, J.W., Kalpana, G.V., Goff, S.P., and Scott, M.P. (1995). The *Drosophila* snr1 and brm proteins are related to yeast SWI/SNF proteins and are components of a large protein complex. Mol. Biol. Cell *6*, 777–791.

Driessens, G., Beck, B., Caauwe, A., Simons, B.D., and Blanpain, C. (2012). Defining the mode of tumour growth by clonal analysis. Nature *488*, 527–530.

Endo, K., Karim, M.R., Taniguchi, H., Krejcí, A., Kinameri, E., Siebert, M., Ito, K., Bray, S.J., and Moore, A.W. (2012). Chromatin modification of Notch targets in olfactory receptor neuron diversification. Nat. Neurosci. *15*, 224–233.

Fog, C.K., Galli, G.G., and Lund, A.H. (2012). PRDM proteins: important players in differentiation and disease. Bioessays *34*, 50–60.

Goardon, N., Marchi, E., Atzberger, A., Quek, L., Schuh, A., Soneji, S., Woll, P., Mead, A., Alford, K.A., Rout, R., et al. (2011). Coexistence of LMPP-like and GMP-like leukemia stem cells in acute myeloid leukemia. Cancer Cell *19*, 138–152.

Gonzalez, C. (2013). *Drosophila melanogaster*: a model and a tool to investigate malignancy and identify new therapeutics. Nat. Rev. Cancer *13*, 172–183.

Harris, R.E., Pargett, M., Sutcliffe, C., Umulis, D., and Ashe, H.L. (2011). Brat promotes stem cell differentiation via control of a bistable switch that restricts BMP signaling. Dev. Cell *20*, 72–83.

Harzer, H., Berger, C., Conder, R., Schmauss, G., and Knoblich, J.A. (2013). FACS purification of *Drosophila* larval neuroblasts for next-generation sequencing. Nat. Protoc. *8*, 1088–1099.

Ho, L., Ronan, J.L., Wu, J., Staahl, B.T., Chen, L., Kuo, A., Lessard, J., Nesvizhskii, A.I., Ranish, J., and Crabtree, G.R. (2009). An embryonic stem cell chromatin remodeling complex, esBAF, is essential for embryonic stem cell self-renewal and pluripotency. Proc. Natl. Acad. Sci. USA *106*, 5181–5186.

Hohenauer, T., and Moore, A.W. (2012). The Prdm family: expanding roles in stem cells and development. Development *139*, 2267–2282.

Homem, C.C., and Knoblich, J.A. (2012). *Drosophila* neuroblasts: a model for stem cell biology. Development *139*, 4297–4310.

Homem, C.C., Reichardt, I., Berger, C., Lendl, T., and Knoblich, J.A. (2013). Long-term live cell imaging and automated 4D analysis of *drosophila* neuroblast lineages. PLoS One *8*, e79588.

Hsu, Y.C., and Fuchs, E. (2012). A family business: stem cell progeny join the niche to regulate homeostasis. Nat. Rev. Mol. Cell Biol. *13*, 103–114.

Jennings, B., Preiss, A., Delidakis, C., and Bray, S. (1994). The Notch signalling pathway is required for Enhancer of split bHLH protein expression during neurogenesis in the *Drosophila* embryo. Development *120*, 3537–3548.

Kadoch, C., Hargreaves, D.C., Hodges, C., Elias, L., Ho, L., Ranish, J., and Crabtree, G.R. (2013). Proteomic and bioinformatic analysis of mammalian SWI/SNF complexes identifies extensive roles in human malignancy. Nat. Genet. *45*, 592–601.

Kidder, B.L., Palmer, S., and Knott, J.G. (2009). SWI/SNF-Brg1 regulates self-renewal and occupies core pluripotency-related genes in embryonic stem cells. Stem Cells *27*, 317–328.

Klein, T., and Campos-Ortega, J.A. (1997). klumpfuss, a *Drosophila* gene encoding a member of the EGR family of transcription factors, is involved in bristle and leg development. Development *124*, 3123–3134.

Kohwi, M., Lupton, J.R., Lai, S.L., Miller, M.R., and Doe, C.Q. (2013). Developmentally regulated subnuclear genome reorganization restricts neural progenitor competence in *Drosophila*. Cell *152*, 97–108.

Krivtsov, A.V., Twomey, D., Feng, Z., Stubbs, M.C., Wang, Y., Faber, J., Levine, J.E., Wang, J., Hahn, W.C., Gilliland, D.G., et al. (2006). Transformation from committed progenitor to leukaemia stem cell initiated by MLL-AF9. Nature *442*, 818–822.

Lee, T., and Luo, L. (1999). Mosaic analysis with a repressible cell marker for studies of gene function in neuronal morphogenesis. Neuron *22*, 451–461.

Lee, T.I., Johnstone, S.E., and Young, R.A. (2006). Chromatin immunoprecipitation and microarray-based analysis of protein location. Nat. Protoc. *1*, 729–748.

Lessard, J.A., and Crabtree, G.R. (2010). Chromatin regulatory mechanisms in pluripotency. Annu. Rev. Cell Dev. Biol. *26*, 503–532.

Lessard, J., Wu, J.I., Ranish, J.A., Wan, M., Winslow, M.M., Staahl, B.T., Wu, H., Aebersold, R., Graef, I.A., and Crabtree, G.R. (2007). An essential switch in subunit composition of a chromatin remodeling complex during neural development. Neuron *55*, 201–215.

Liu, C., and Zong, H. (2012). Developmental origins of brain tumors. Curr. Opin. Neurobiol. *22*, 844–849.

Liu, C., Sage, J.C., Miller, M.R., Verhaak, R.G., Hippenmeyer, S., Vogel, H., Foreman, O., Bronson, R.T., Nishiyama, A., Luo, L., and Zong, H. (2011). Mosaic analysis with double markers reveals tumor cell of origin in glioma. Cell *146*, 209–221.

Livak, K.J., and Schmittgen, T.D. (2001). Analysis of relative gene expression data using real-time quantitative PCR and the 2(-Δ Δ C(T)) Method. Methods *25*, 402–408.

Lui, J.H., Hansen, D.V., and Kriegstein, A.R. (2011). Development and evolution of the human neocortex. Cell *146*, 18–36.

Ma, Y., Niemitz, E.L., Nambu, P.A., Shan, X., Sackerson, C., Fujioka, M., Goto, T., and Nambu, J.R. (1998). Gene regulatory functions of *Drosophila* fish-hook, a high mobility group domain Sox protein. Mech. Dev. *73*, 169–182.

Matsumoto, S., Banine, F., Struve, J., Xing, R., Adams, C., Liu, Y., Metzger, D., Chambon, P., Rao, M.S., and Sherman, L.S. (2006). Brg1 is required for murine neural stem cell maintenance and gliogenesis. Dev. Biol. *289*, 372–383.

Maurange, C., Cheng, L., and Gould, A.P. (2008). Temporal transcription factors and their targets schedule the end of neural proliferation in *Drosophila*. Cell *133*, 891–902.

McGuire, S.E., Mao, Z., and Davis, R.L. (2004). Spatiotemporal gene expression targeting with the TARGET and gene-switch systems in *Drosophila*. Sci. STKE *2004*, pl6.

Mohrmann, L., and Verrijzer, C.P. (2005). Composition and functional specificity of SWI2/SNF2 class chromatin remodeling complexes. Biochim. Biophys. Acta *1681*, 59–73.

Moore, A.W., Jan, L.Y., and Jan, Y.N. (2002). hamlet, a binary genetic switch between single- and multiple- dendrite neuron morphology. Science *297*, 1355–1358.

Moore, A.W., Roegiers, F., Jan, L.Y., and Jan, Y.N. (2004). Conversion of neurons and glia to external-cell fates in the external sensory organs of *Drosophila* hamlet mutants by a cousin-cousin cell-type respecification. Genes Dev. *18*, 623–628.

Moshkin, Y.M., Mohrmann, L., van Ijcken, W.F., and Verrijzer, C.P. (2007). Functional differentiation of SWI/SNF remodelers in transcription and cell cycle control. Mol. Cell. Biol. *27*, 651–661.

Neumüller, R.A., Richter, C., Fischer, A., Novatchkova, M., Neumüller, K.G., and Knoblich, J.A. (2011). Genome-wide analysis of self-renewal in *Drosophila* neural stem cells by transgenic RNAi. Cell Stem Cell *8*, 580–593.

Northcott, P.A., Jones, D.T.W., Kool, M., Robinson, G.W., Gilbertson, R.J., Cho, Y.-J., Pomeroy, S.L., Korshunov, A., Lichter, P., Taylor, M.D., and Pfister, S.M. (2012). Medulloblastomics: the end of the beginning. Nat. Rev. Cancer *12*, 818–834.

Parrish, J.Z., Kim, M.D., Jan, L.Y., and Jan, Y.-N. (2006). Genome-wide analyses identify transcription factors required for proper morphogenesis of *Drosophila* sensory neuron dendrites. Genes Dev. *20*, 820–835.

Parsons, D.W., Li, M., Zhang, X., Jones, S., Leary, R.J., Lin, J.C.-H., Boca, S.M., Carter, H., Samayoa, J., Bettegowda, C., et al. (2011). The genetic landscape of the childhood cancer medulloblastoma. Science *331*, 435–439.

Pfeiffer, B.D., Jenett, A., Hammonds, A.S., Ngo, T.T., Misra, S., Murphy, C., Scully, A., Carlson, J.W., Wan, K.H., Laverty, T.R., et al. (2008). Tools for neuroanatomy and neurogenetics in *Drosophila*. Proc. Natl. Acad. Sci. USA *105*, 9715–9720.

Pinheiro, I., Margueron, R., Shukeir, N., Eisold, M., Fritzsch, C., Richter, F.M., Mittler, G., Genoud, C., Goyama, S., Kurokawa, M., et al. (2012). Prdm3 and Prdm16 are H3K9me1 methyltransferases required for mammalian heterochromatin integrity. Cell *150*, 948–960.

Reichert, H. (2011). *Drosophila* neural stem cells: cell cycle control of self-renewal, differentiation, and termination in brain development. Results Probl. Cell Differ. *53*, 529–546.

Reisman, D., Glaros, S., and Thompson, E.A. (2009). The SWI/SNF complex and cancer. Oncogene *28*, 1653–1668.

Richter, C., Oktaba, K., Steinmann, J., Müller, J., and Knoblich, J.A. (2011). The tumour suppressor L(3)mbt inhibits neuroepithelial proliferation and acts on insulator elements. Nat. Cell Biol. *13*, 1029–1039.

Ronan, J.L., Wu, W., and Crabtree, G.R. (2013). From neural development to cognition: unexpected roles for chromatin. Nat. Rev. Genet. *14*, 347–359.

Russell, S.R., Sanchez-Soriano, N., Wright, C.R., and Ashburner, M. (1996). The Dichaete gene of *Drosophila melanogaster* encodes a SOX-domain protein required for embryonic segmentation. Development *122*, 3669–3676.

San-Juán, B.P., and Baonza, A. (2011). The bHLH factor deadpan is a direct target of Notch signaling and regulates neuroblast self-renewal in *Drosophila*. Dev. Biol. *352*, 70–82.

Sarkar, A., and Hochedlinger, K. (2013). The sox family of transcription factors: versatile regulators of stem and progenitor cell fate. Cell Stem Cell *12*, 15–30.

Schepers, A.G., Snippert, H.J., Stange, D.E., van den Born, M., van Es, J.H., van de Wetering, M., and Clevers, H. (2012). Lineage tracing reveals Lgr5+ stem cell activity in mouse intestinal adenomas. Science *337*, 730–735.

Schober, M., Schaefer, M., and Knoblich, J.A. (1999). Bazooka recruits Inscuteable to orient asymmetric cell divisions in *Drosophila* neuroblasts. Nature *402*, 548–551.

Schüller, U., Heine, V.M., Mao, J., Kho, A.T., Dillon, A.K., Han, Y.G., Huillard, E., Sun, T., Ligon, A.H., Qian, Y., et al. (2008). Acquisition of granule neuron precursor identity is a critical determinant of progenitor cell competence to form Shh-induced medulloblastoma. Cancer Cell *14*, 123–134.

Schwitalla, S., Fingerle, A.A., Cammareri, P., Nebelsiek, T., Göktuna, S.I., Ziegler, P.K., Canli, O., Heijmans, J., Huels, D.J., Moreaux, G., et al. (2013). Intestinal tumorigenesis initiated by dedifferentiation and acquisition of stem-cell-like properties. Cell *152*, 25–38.

Seo, S., Richardson, G.A., and Kroll, K.L. (2005). The SWI/SNF chromatin remodeling protein Brg1 is required for vertebrate neurogenesis and mediates transactivation of Ngn and NeuroD. Development *132*, 105–115.

Shain, A.H., and Pollack, J.R. (2013). The spectrum of SWI/SNF mutations, ubiquitous in human cancers. PLoS One *8*, e55119.

Song, Y., and Lu, B. (2011). Regulation of cell growth by Notch signaling and its differential requirement in normal vs. tumor-forming stem cells in *Drosophila*. Genes Dev. *25*, 2644–2658.

Sonoda, J., and Wharton, R.P. (2001). *Drosophila* brain tumor is a translational repressor. Genes Dev. *15*, 762–773.

Southall, T.D., and Brand, A.H. (2009). Neural stem cell transcriptional networks highlight genes essential for nervous system development. EMBO J. *28*, 3799–3807.

Tamkun, J.W., Deuring, R., Scott, M.P., Kissinger, M., Pattatucci, A.M., Kaufman, T.C., and Kennison, J.A. (1992). brahma: a regulator of *Drosophila* homeotic genes structurally related to the yeast transcriptional activator SNF2/SWI2. Cell *68*, 561–572.

Tea, J.S., and Luo, L. (2011). The chromatin remodeling factor Bap55 functions through the TIP60 complex to regulate olfactory projection neuron dendrite targeting. Neural Dev. *6*, 5.

Towbin, B.D., González-Aguilera, C., Sack, R., Gaidatzis, D., Kalck, V., Meister, P., Askjaer, P., and Gasser, S.M. (2012). Step-wise methylation of histone H3K9 positions heterochromatin at the nuclear periphery. Cell *150*, 934–947.

Treisman, J.E., Luk, A., Rubin, G.M., and Heberlein, U. (1997). eyelid antagonizes wingless signaling during *Drosophila* development and has homology to the Bright family of DNA-binding proteins. Genes Dev. *11*, 1949–1962.

Truman, J.W., and Bate, M. (1988). Spatial and temporal patterns of neurogenesis in the central nervous system of *Drosophila melanogaster*. Dev. Biol. *125*, 145–157.

Tuoc, T.C., Boretius, S., Sansom, S.N., Pitulescu, M.E., Frahm, J., Livesey, F.J., and Stoykova, A. (2013). Chromatin regulation by BAF170 controls cerebral cortical size and thickness. Dev. Cell *25*, 256–269.

Vaessin, H., Grell, E., Wolff, E., Bier, E., Jan, L.Y., and Jan, Y.N. (1991). prospero is expressed in neuronal precursors and encodes a nuclear protein that is involved in the control of axonal outgrowth in *Drosophila*. Cell *67*, 941–953.

Vázquez, M., Moore, L., and Kennison, J.A. (1999). The trithorax group gene osa encodes an ARID-domain protein that genetically interacts with the brahma chromatin-remodeling factor to regulate transcription. Development *126*, 733–742.

Weng, M., and Lee, C.Y. (2011). Keeping neural progenitor cells on a short leash during *Drosophila* neurogenesis. Curr. Opin. Neurobiol. *21*, 36–42.

Weng, M., Golden, K.L., and Lee, C.Y. (2010). dFezf/Earmuff maintains the restricted developmental potential of intermediate neural progenitors in *Drosophila*. Dev. Cell *18*, 126–135.

Wilson, B.G., and Roberts, C.W. (2011). SWI/SNF nucleosome remodellers and cancer. Nat. Rev. Cancer *11*, 481–492.

Wu, J.I., Lessard, J., Olave, I.A., Qiu, Z., Ghosh, A., Graef, I.A., and Crabtree, G.R. (2007). Regulation of dendritic development by neuron-specific chromatin remodeling complexes. Neuron *56*, 94–108.

Wu, J.I., Lessard, J., and Crabtree, G.R. (2009). Understanding the words of chromatin regulation. Cell *136*, 200–206.

Xiao, Q., Komori, H., and Lee, C.-Y. (2012). klumpfuss distinguishes stem cells from progenitor cells during asymmetric neuroblast division. Development *139*, 2670–2680.

Yang, Z.J., Ellis, T., Markant, S.L., Read, T.A., Kessler, J.D., Bourboulas, M., Schüller, U., Machold, R., Fishell, G., Rowitch, D.H., et al. (2008). Medulloblastoma can be initiated by deletion of Patched in lineage-restricted progenitors or stem cells. Cancer Cell *14*, 135–145.

Yoo, A.S., and Crabtree, G.R. (2009). ATP-dependent chromatin remodeling in neural development. Curr. Opin. Neurobiol. *19*, 120–126.

Yuzyuk, T., Fakhouri, T.H.I., Kiefer, J., and Mango, S.E. (2009). The polycomb complex protein mes-2/E(z) promotes the transition from developmental plasticity to differentiation in *C. elegans* embryos. Dev. Cell *16*, 699–710.

Zacharioudaki, E., Magadi, S.S., and Delidakis, C. (2012). bHLH-O proteins are crucial for *Drosophila* neuroblast self-renewal and mediate Notch-induced overproliferation. Development *139*, 1258–1269.

Zeng, X., Lin, X., and Hou, S.X. (2013). The Osa-containing SWI/SNF chromatin-remodeling complex regulates stem cell commitment in the adult *Drosophila* intestine. Development *140*, 3532–3540.

Zhu, S., Lin, S., Kao, C.F., Awasaki, T., Chiang, A.S., and Lee, T. (2006). Gradients of the *Drosophila* Chinmo BTB-zinc finger protein govern neuronal temporal identity. Cell *127*, 409–422.

Zhu, S., Barshow, S., Wildonger, J., Jan, L.Y., and Jan, Y.N. (2011). Ets transcription factor Pointed promotes the generation of intermediate neural progenitors in *Drosophila* larval brains. Proc. Natl. Acad. Sci. USA *108*, 20615–20620.